Critical roles for collagenase-3 (Mmp13) in development of growth plate cartilage and in endochondral ossification

Masaki Inada*†, Yingmin Wang*†, Michael H. Byrne*, Mahboob U. Rahman*, Chisato Miyaura‡, Carlos López-Otín§, and Stephen M. Krane*¶

*Center for Immunology and Inflammatory Diseases, Department of Medicine, Harvard Medical School and Massachusetts General Hospital, Building 149, 13th Street, Room 8301, Boston, MA 02129; ‡Department of Biotechnology and Life Science, Tokyo University of Agriculture and Technology, Nakamachi, Koganei, Tokyo 184-8588, Japan; and §Departamento de Bioquimica y Biología Molecular, Instituto Universitario de Oncologia, Universidad de Oviedo, 33006 Oviedo, Spain

Communicated by Leon E. Rosenberg, Princeton University, Princeton, NJ, October 20, 2004 (received for review July 13, 2004)

Collagenase-3 (MMP13), a member of the matrix metalloproteinase (MMP) family of neutral endopeptidases, is expressed in the skeleton during embryonic development and is highly overexpressed in human carcinomas and in chondrocytes and synovial cells in rheumatoid arthritis and osteoarthritis. To determine the functional roles of Mmp13, we generated *Mmp13*-null mice that showed profound defects in growth plate cartilage with markedly increased hypertrophic domains as well as delay in endochondral ossification and formation and vascularization of primary ossification centers. Absence of Mmp13 resulted in significant interstitial collagen accumulation due, in part, to the lack of appropriate collagenase-mediated cleavage that normally occurs in growth plates and primary ossification centers. Cartilaginous growth plate abnormalities persisted in adult mice and phenocopied defects observed in human hereditary chondrodysplasias. Our findings demonstrate a unique role of Mmp13 in skeletal development.

collagen | extracellular matrix | vascularization

Collagenases, a group of matrix metalloproteinases (MMPs) that act at neutral pH (1–4), have been postulated to have a role in skeletal development and bone remodeling (5–8). The MMPs are members of a large family of proteinases that have several structural features in common including the presence of a conserved zinc-binding catalytic domain (1–4). Only the products of specific MMP genes, *MMP1*, *-2*, *-8*, *-13*, and *-14*, however, have the capacity to cleave native, undenatured, interstitial collagens at a specific helical locus (9–13). Of the collagenases, MMP13 (collagenase-3) has been considered to have an important role in skeletal biology in view of its exclusive presence in the skeleton during embryonic development in cartilaginous growth plates and primary centers of ossification (5–8). *MMP13* is also a downstream target of parathyroid hormone (PTH)-related protein (PTHrP) (14) and the transcription factor *Osf2/Cbfa1/Runx2* in growth plate chondrocytes (15, 16). In contrast to humans, where *MMP1* may be strongly expressed, e.g., in inflammation, the orthologue of *MMP1*, McolA (12), is expressed in mice only at low levels.

To examine possible functional roles of collagenases during skeletal development *in vivo*, we targeted a null mutation to the Mmp13 gene in mice. Our targeting strategy resulted in splicing out exon 5 that encodes the zinc-binding residues in the catalytic domain. As described here, deletion of functional Mmp13 had profound effects on skeletal development. In *Mmp13*$^{-/-}$ embryos compared with WT embryos, the growth plates were strikingly lengthened, a defect ascribable predominantly to a delay in terminal events in the growth plates, with failure to resorb collagens, as well as a delay in ossification at the primary centers.

Materials and Methods

Generation of *Mmp13*$^{-/-}$ Mice. We isolated two *Mmp13* genomic clones from a 129/J1 library to construct the knockout vector. The first was a *Bam*HI/*Sal*I fragment that spanned from ≈3.4 kb of promoter sequence through the first ≈1.4 kb of intron 4, cloned into pT7Blue-3. A PGK*neo* cassette was inserted between *Sal*I and *Xba*I sites that resulted from the cloning. The second genomic clone served as template for PCR with primers in intron 4 and exon 9 that included new *Xba*I sites to serve as the 3′ arm (≈4.5 kb) of the final construct. The forward primer also contained sequences of the intron 4/exon 5 junction followed by codons for the first two amino acids (YN), a TAA stop codon with the last 2 bp of the F262 codon deleted, altering the coding for the critical zinc-binding sequences in the catalytic domain. This targeting construct thus encodes a truncated protein, but during transcription, exon 5 might be spliced out.

For gene targeting, the knockout vector was purified and two clones were linearized in the 5′ or 3′ polylinker and electroporated into J1 embryonic stem (ES) cells. With the vector linearized at the 5′ end, of 200 G418-resistant clones screened by PCR, seven had correct integration, confirmed in four by Southern blotting. With the vector linearized at the 3′ end, four clones had correct integration. ES cells with correct integration were injected into C57BL/6 blastocysts, and overtly chimeric males were obtained and mated with WT C57BL/6 females. DNA from tail snips of agouti offspring was analyzed by PCR and Southern blotting. Germline transmission was successful when using each of the two independently derived ES cell clones and resulted in similar phenotypes.

Tissue Processing and Analysis. Mice were killed by CO_2 narcosis to obtain tissue. Bones were removed, cleaned, fixed in 10% phosphate-buffered formalin, decalcified in 14% EDTA, and dehydrated in graded alcohol for paraffin embedding. Longitudinal 5-μm sections were prepared from embryos and newborns through the epiphyses and shafts of long bones. Femurs from adult mice were fixed in 70% ethanol and embedded in glycol methacrylate, and undecalcified 3-μm sections were stained with toluidene blue.

Immunohistochemistry and Immunoblotting. Antibodies used for immunohistochemistry and Western blotting were as follows. A rabbit polyclonal antibody to the N-terminal neoepitope QRGIV (amino acids 779–783) in the collagenase cleavage C-terminal 1/4 fragment ($B^{\alpha 1[II]}$) of mouse and chick type II collagen and QRGVV in $B^{\alpha 1[I]}$ of type I collagen was generously provided by Eunice Lee (Shriners Hospital for Children, Mon-

Abbreviations: dpc, days postconception; ECM, extracellular matrix; PTH, parathyroid hormone; TRAP, tartrate resistant acid phosphatase.

†M.I. and Y.W. contributed equally to this work.

¶To whom correspondence should be addressed. E-mail: krane.stephen@mgh.harvard.edu.

treal). Epitope specificity of the antibody to QRGIV was demonstrated in Western blots of collagenase-digested collagens. Type I collagen was extracted and purified from mouse skin (17), and chick type II collagen was from Sigma. Human *MMP13* cDNA in the pcDNA 3.1 vector was transfected into human embryonic kidney (HEK) 293 cells, and conditioned medium was harvested. Collagenase digestion and analysis was performed as described in ref. 17; proMMP13 was activated by using 1 mM *p*-aminophenylmercuric acetate. The mouse mAb 9A4 (18), which detects a C-terminal neoepitope (amino acids 769–775) in collagenase-cleaved collagens [in the α 1(II) chains of type II collagen and in the α 1(I) chains of type I collagen], was generously provided by Ivan Otterness (Central Research Division, Pfizer, Groton, CT) and was used as described in ref. 19. The rabbit polyclonal antibody against the C-terminal domain of mouse type X collagen was generously provided by Bjorn Olsen (Harvard Medical School). The rabbit polyclonal antibody to CD31 was from Santa Cruz Biotechnology.

Aliquots of conditioned medium of calvarial cultures or Mmp13 digests of mouse type I and chick type II collagens were resolved by SDS/PAGE with 10% polyacrylamide gels (17), and the proteins were transferred to polyvinylidene difluoride membranes (Hybond-P, Amersham Biosciences). After blocking for 1 h with 5% nonfat dry milk in PBS/0.1% Tween 20 at 4°C, membranes were incubated for 2 h with an anti-Mmp13 mAb (Chemicon). After incubation with horseradish peroxidase-conjugated rabbit anti-mouse IgG for 1 h, immunoreactive bands were detected by using an ECL system (Amersham Biosciences).

For tissue immunohistochemistry, paraffin sections were rehydrated with graded alcohol and blocked with 5% nonfat dry milk for 30 min, and primary antibodies were applied for 2 h. After incubation with biotin-conjugated secondary antibody for 1 h, sections were reacted either with the AEC substrate kit for peroxidase (Vector Laboratories) for light microscopy or with streptavidin-conjugated Alexa Fluor 568 (Molecular Probes) for fluorescence microscopy. Images were obtained by using a Nikon metallurgical microscope (Nikon, Melville, NY) and recorded by using the SPOT RT Slider digital camera system (Diagnostic Instruments, Sterling Heights, MI).

***In Situ* Hybridization and RNA Analysis.** Paraffin sections were used for *in situ* hybridization with uridine 5′-[α-^{35}S]thiotriphosphate-labeled antisense riboprobes (Amersham Biosciences) (20). Two different Mmp13 cRNA probes were used: 5′probe, bp 1–695; exon 5 probe, bp 627–816 (GenBank accession no. NM_008607). RNA was isolated from distal femurs and proximal tibias, including knee joints, and analyzed by Northern blotting (21, 22). Quantification of mRNA levels was achieved by real-time PCR with either TaqMan probes or SYBR Green and the ABI Prism 7700 sequence detector (Applied Biosystems). Standard curves for each gene were established by using cDNA templates. Primer sequences are available on request.

Calvarial Organ Cultures. Calvariae from 5-day-old mice were isolated aseptically, cleaned, and cultured for 16 h at 37°C under 5% CO_2 in air in 0.5 ml of BGJb medium (Life Technologies) containing 1 mg/ml BSA (fraction V, Sigma) (21, 22). Half calvariae were transferred to fresh medium with or without 0.1 μM PTH or 1 nM IL-1α and cultured for an additional 5 days. Conditioned medium was collected for analysis by Western blotting, and RNA was extracted from tissue for Northern blotting and quantification by real-time PCR.

Statistical Analysis. Some data are expressed as means ± SEM. Significance of differences was analyzed by using Student's *t* test.

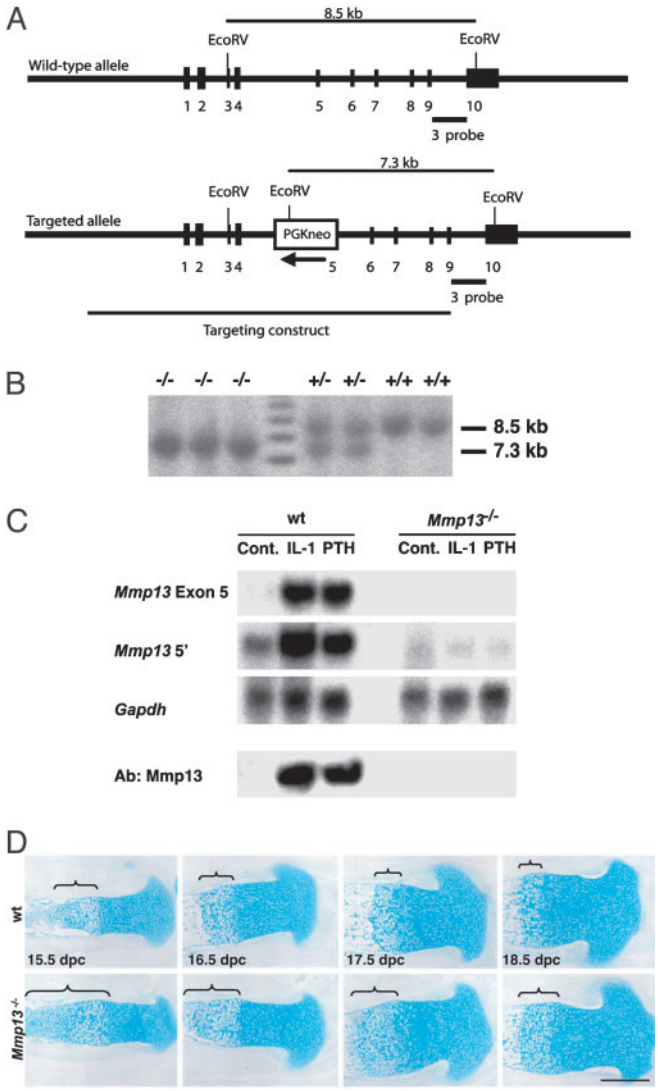

Fig. 1. Generation of *Mmp13*$^{-/-}$ mice. (*A*) Schematic representation of the WT *Mmp13* locus, the targeting vector, the targeted allele, the position of *Eco*RV sites, and the probe used for Southern blot analysis. (*B*) Southern blot analysis of genomic DNA from littermate progeny of *Mmp13*$^{+/-}$ breeding. Probes of *Eco*RV-digested DNA identified the fragments of 8.5 and 7.3 kb for WT and disrupted alleles, respectively. (*C*) Northern blot analysis of calvarial RNA after calvarial organ cultures for 5 days with or without IL-1α or PTH, and Western blot analysis of conditioned medium from these organ cultures. Levels of *Mmp13* mRNA increased in WT calvariae exposed to IL-1α or PTH in contrast with *Mmp13*$^{-/-}$ calvariae. A marked increase in Mmp13 (Ab:Mmp13) is seen in Western blots from WT calvarial conditioned medium, but no increase in Mmp13 is seen in *Mmp13*$^{-/-}$ calvarial conditioned medium. (*D*) Skeletal development in WT and *Mmp13*$^{-/-}$ 15.5- to 18.5-dpc embryos. Sections of proximal tibias were stained with Alcian blue. Increases in length of the hypertrophic zones of the growth plates, indicated by the brackets, are seen in the *Mmp13*$^{-/-}$ tibias. (Scale bar: 400 μm.)

Results

***Mmp13*-Null Mutation.** The proportion of WT (+/+), *Mmp13*$^{+/-}$, and *Mmp13*$^{-/-}$ embryos, based on Southern blot (Fig. 1 *A* and *B*) and PCR analysis, was consistent with Mendelian predictions. Newborn *Mmp13*$^{-/-}$ mice appeared healthy. To assess transcription of mutant *Mmp13*, total RNA extracted from calvariae of 5-day-old mice was analyzed by RT-PCR with primers that spanned from exon 4 to exon 7. We found a single band of ≈430 bp, as predicted, in WT calvariae but a band of only ≈268 bp in

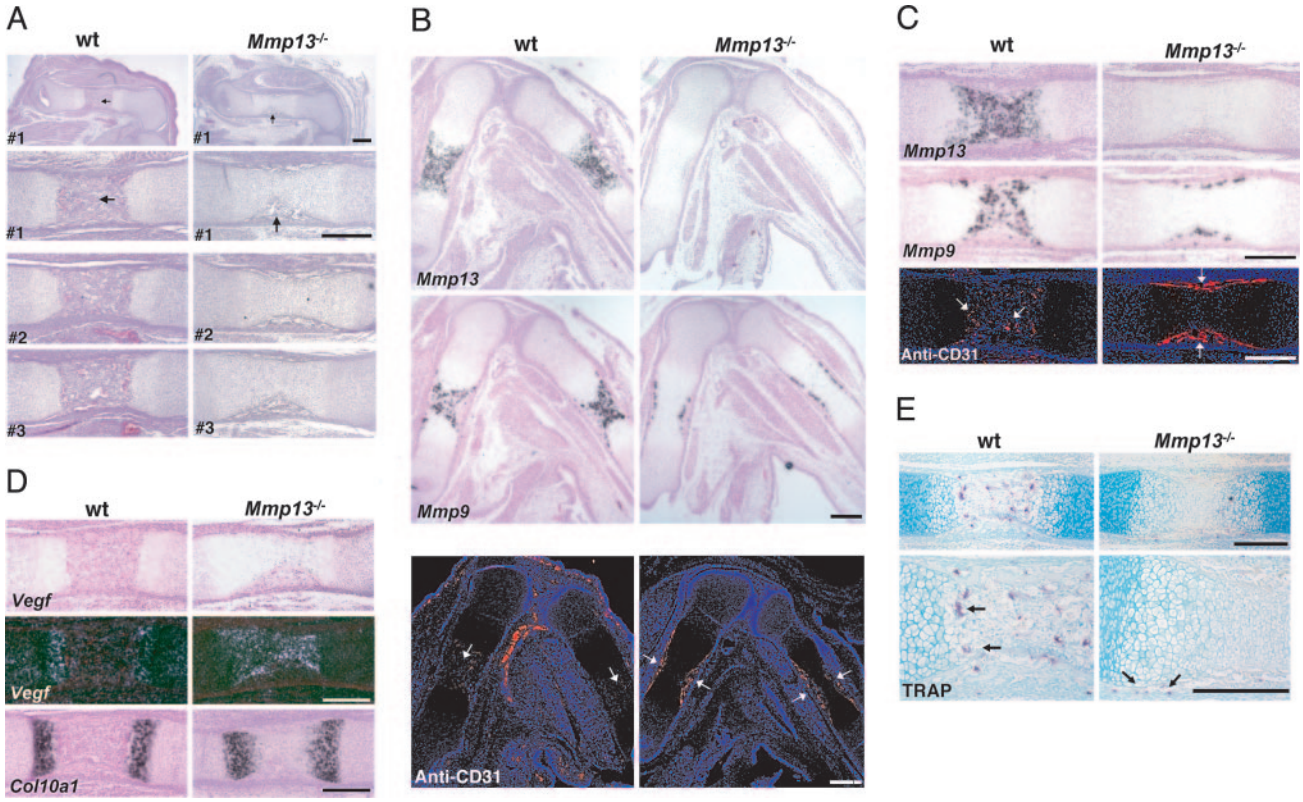

Fig. 2. Analysis of long bones from WT and *Mmp13*$^{-/-}$ mice. (*A*) Sections of femurs from three different WT and *Mmp13*$^{-/-}$ 15.5-dpc embryos stained with hematoxylin/eosin. The top panels are low-power views, and the other panels are higher-power views. Primary ossification centers are fully formed in WT samples, but only periosteal cuffs (arrows) are fully formed in *Mmp13*$^{-/-}$ samples. (Scale bar: 300 μm.) (*B*) Adjacent sections of femurs and tibias from 15.5-dpc embryos. *In situ* hybridization was used for analysis of *Mmp13* and *-9* mRNAs, and immunohistochemistry was used for analysis of CD31 (seen as red on blue-black background). Note CD31 (arrows) in primary centers of WT bones but restricted to periosteal cuffs in *Mmp13*$^{-/-}$ bones. (Scale bar: 300 μm.) (*C*) Higher-power images of mid-femurs shown in *B*. (Scale bar: 300 μm.) (*D*) Mid-femurs as in *C*. *In situ* hybridization was used for analysis of *Vegf* and *Col10a1* mRNAs. (Scale bar: 300 μm.) (*E*) Mid-femurs as in *A* stained for TRAP. Note the TRAP^{+} cells (arrows). (Scale bar: 300 μm.)

Mmp13$^{-/-}$ calvariae, consistent with a transcript lacking exon 5 (confirmed by DNA sequencing). No band of 333 bp corresponding to a TAA stop codon-truncated exon 5 was detected. We expressed in *E. coli* a *Mmp13* cDNA with exon 5 sequences deleted and found it to be devoid of collagenase activity (data not shown).

Levels of *Mmp13* mRNA increased markedly in cultured WT calvariae incubated either with IL-1α or PTH (Fig. 1*C*). In contrast, there was no detectable *Mmp13* mRNA in *Mmp13*$^{-/-}$ calvariae when using the exon 5 probe and barely detectable mRNA when using the 5′ probe. Western blots of conditioned medium showed a marked increase in Mmp13 levels induced by PTH or IL-1α in cultures of WT calvariae; no Mmp13 was detected in medium from cultures of *Mmp13*$^{-/-}$ calvariae (Fig. 1*C*). The antibody used in these assays recognizes *Escherichia coli*-expressed mutant (exon 5 deleted) Mmp13.

Abnormalities of the Limb Growth Plates and Delay in Ossification in *Mmp13*$^{-/-}$ Mice. In sections of long bones from hind limbs (Fig. 1*D*), the length of the growth plates in *Mmp13*$^{-/-}$ embryos was increased compared with *Mmp13*$^{+/-}$ or WT embryos and was maintained throughout development. The length of the total growth plate in proximal tibias (measured from articular surface to primary spongiosa) was increased in *Mmp13*$^{-/-}$ embryos vs. WT embryos by ≈20% and that of the hypertrophic zone by ≈70%. In addition, the chondrocyte columns in *Mmp13*$^{-/-}$ mice were less well aligned and were disordered compared with those in WT mice. These abnormalities persisted in newborns and adults and were still evident in 4-month-old mice.

There was a profound delay in development of the primary ossification centers in *Mmp13*$^{-/-}$ mice. In 15.5-dpc WT embryos (dpc, days postconception), primary ossification centers were fully formed in femurs and tibias (Fig. 2*A*), in contrast with *Mmp13*$^{-/-}$ embryos, where primary centers were not formed and only a diaphyseal periosteal collar was visible. In adjacent sections (Fig. 2 *B* and *C*), *Mmp13* expression was prominent in the primary ossification centers in WT embryos but was not detected in *Mmp13*$^{-/-}$ embryos. The pattern of immunostaining for CD31, an endothelial cell marker, in WT embryos correlated with that of *Mmp13* expression, i.e., prominent within the well formed primary ossification centers. Staining was limited to the periosteal collar, however, in the *Mmp13*$^{-/-}$ embryos (Fig. 2 *B* and *C*). Osteoclasts that express tartrate resistant acid phosphatase (TRAP) as well as *Mmp9* are apparently important in initial phases of development of primary ossification centers (23). In 15.5-dpc embryos, the pattern of *Mmp9* (Fig. 2 *B* and *C*) expression in WT and *Mmp13*$^{-/-}$ embryos mirrored that of CD31. Abundant TRAP^{+} osteoclasts (Fig. 2*E*) were present in WT ossification centers, but TRAP^{+} cells were limited to the diaphyseal collar in *Mmp13*$^{-/-}$ mice. In *Mmp13*$^{-/-}$ mice, impaired vascularization (shown by CD31 staining) correlated with the defect in development of primary ossification centers and the absence of *Mmp13*; expression of Mmp9 (24) limited to the periosteal cuff did not compensate for the absence of Mmp13.

Nevertheless, by 17.5 dpc, when growth plates were still lengthened, primary ossification centers had formed and abundant TRAP^{+} cells were found there in *Mmp13*$^{-/-}$ and WT mice (arrows in Fig. 3) and were particularly prominent in the primary

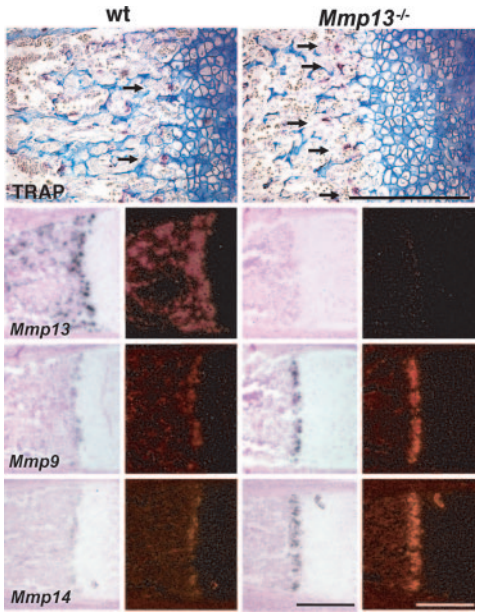

Fig. 3. Proximal tibias from 17.5-dpc embryos showing TRAP$^+$ cells (arrows) and analysis by *in situ* hybridization for *Mmp13*, *-9*, and *-14* mRNAs. (Scale bar: 300 μm.)

spongiosa near the edge of the cartilaginous growth plates where *Mmp9* was also highly expressed. Osteoclasts express *Mmp14* (*MT1-Mmp*) as well, and *Mmp14*$^{-/-}$ mice have defects in endochondral ossification (25, 26). In our studies, *Mmp14* was expressed in 17.5-dpc embryos in a pattern similar to that of TRAP and *Mmp9* with higher levels in the *Mmp13*$^{-/-}$ bones compared with WT bones (Fig. 3). Collagenase-2 (*Mmp8*) was not detected in 15.5- or 17.5-dpc WT embryos but was expressed at low levels in distal growth plates and primary centers of ossification of 15.5- and 17.5-dpc *Mmp13*$^{-/-}$ embryos (data not shown). In newborn WT mice, expression of *Mmp8* was noted in bone marrow cavities; levels higher than in WT were observed in newborn *Mmp13*$^{-/-}$ mice (data not shown). Using real-time PCR with RNA extracted from the distal femurs and proximal tibias of newborn WT and *Mmp13*$^{-/-}$ mice, *Mmp8* mRNA levels were higher in *Mmp13*$^{-/-}$ mice than in WT mice (mean 12.6 vs. 6.8 $\times$ 10^3 molecules per ng of RNA). *Mmp9* mRNA levels were also higher in *Mmp13*$^{-/-}$ than in WT mice (mean 3.6 vs. 2.2 $\times$ 10^4 molecules per ng of RNA), consistent with the results obtained by *in situ* hybridization.

Extracellular Matrix (ECM) Proteins in Endochondral Ossification. Type X collagen is normally produced only by hypertrophic chondrocytes in the distal growth plate (27, 28), and mutations in *Col10a1* cause chondrodysplasias (28). As shown in Fig. 2*D*, in 15.5-dpc embryos and in Fig. 4*A*, in newborns, there was comparable intensity of expression of *Col10a1* in growth plates from WT and *Mmp13*$^{-/-}$ mice. The anatomic domain where *Col10a1* was expressed, however, was increased in *Mmp13*$^{-/-}$ mice vs. WT mice, corresponding to the increase in length of the zone of hypertrophy and consistent with increased numbers of hypertrophic chondrocytes in *Mmp13*$^{-/-}$ mice vs. WT mice. There was also a striking increase in the domain where type X collagen was deposited (immunohistochemistry) in the growth plates in *Mmp13*$^{-/-}$ mice vs. WT mice (Fig. 4*B*). The increase in deposition of type X collagen in the *Mmp13*$^{-/-}$ embryos could thus be due to decreased resorption (lack of collagenase) or increased synthesis. The domain of expression of osteopontin, another marker of chondrocyte hypertrophy (29, 30), was also increased in the distal growth plates from the *Mmp13*$^{-/-}$ mice vs. WT mice (Fig. 4*A*), consistent with the observed increase in hypertrophic chondrocytes and delay in ossification.

We provide evidence that *Mmp13* expressed in distal growth plates and primary ossification centers normally functions in collagen degradation. Staining with the antibody that detects the QRGIV sequence in the C-terminal (TC^B) type II collagen fragment was observed in distal growth plates in WT mice (Fig. 4*B*). This antibody also detects the QRGVV epitope in the TC$^{B\alpha1(I)}$ type I collagen fragment (Fig. 4*B*), which can account for staining also observed in the WT primary ossification centers. In contrast, no staining was detected in distal growth plates from *Mmp13*$^{-/-}$ mice and only faint staining was detected in the bone marrow cavities where other *Mmp*s, e.g., *Mmp8*, are also expressed, particularly after birth when these cavities are populated by *Mmp8*-expressing hematopoietic cells. Staining with mAb 9A4 (18) that detects sequences in TC^A type II collagenolytic fragments was seen in the intercellular septae of distal growth plates and primary centers from newborn WT mice but not from *Mmp13*$^{-/-}$ mice (data not shown). Lack of staining with antibody to QRGIV and mAb 9A4 in growth plates from *Mmp13*$^{-/-}$ mice suggests that Mmp13 is normally the collagenase responsible for collagen degradation in growth plate cartilage during endochondral ossification.

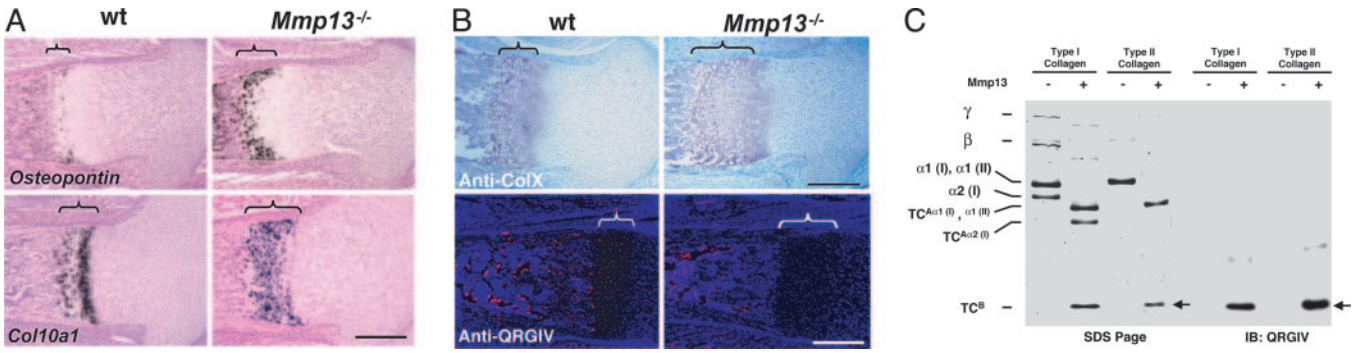

Fig. 4. Analysis of tibias and femurs. (*A*) *In situ* hybridization for *Osteopontin* and *Col10a1* mRNAs in proximal tibias from 18.5-dpc embryos. Brackets indicate the lengths of hypertrophic zones. (Scale bar: 300 μm.) (*B*) Proximal femurs from newborn (P0) mice. Sections were stained for type X collagen and for QRGIV epitope in collagenolytic TC^B fragments. Brackets indicate the lengths of hypertrophic zones. Note the absence of anti-QRGIV staining [shown as red on blue-black background] in distal growth plates and primary centers of *Mmp13*$^{-/-}$ bones. (Scale bar: 300 μm.) (*C*) SDS/PAGE stained with Coomassie blue (left) and Western blots (right) of collagenase (MMP13) digests of types I and II collagens. The TC$^{B\alpha\ 1}$ fragments are indicated by arrows. The faster-moving TC$^{B\alpha2(I)}$ fragment of type I collagen moved off the gel. The QRGIV antibody, which detects the neoepitope in the TC$^{B\alpha\ 1(I)}$ and TC$^{B\alpha\ 1(II)}$ collagenase-cleavage fragments of types I and II collagens, respectively, was used in the immunoblots (IB:QRGIV).

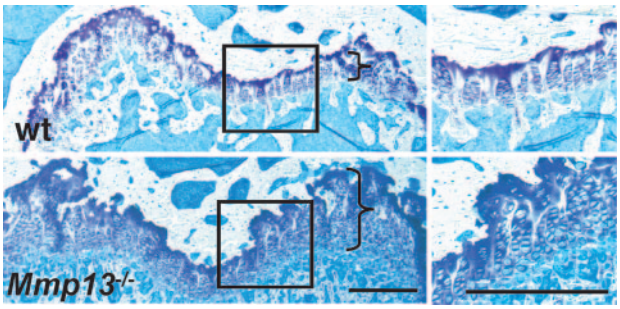

Fig. 5. Sections of distal femoral growth plates from 12-wk-old WT and *Mmp13*$^{-/-}$ mice. Brackets indicate the approximate lengths of the growth plates. Higher-magnification views of the boxed areas in *Left* are shown in *Right*. Note the increased lengths of the growth plates and the irregular arrangement of the chondrocyte columns in *Mmp13*$^{-/-}$ samples vs. WT samples. (Scale bar: 300 μm.)

Expression of Regulatory Genes in Growth Plates and Primary Ossification Centers. Intensity of expression by *in situ* hybridization of PTH/PTHrP receptor, Indian hedgehog, and its receptor, patched, all regulatory factors in developing growth plates (31, 32), was similar in WT and *Mmp13*$^{-/-}$ mice (data not shown). Because vascularization and influx of osteogenic cells from the primary center of ossification are determinants of the length of the hypertrophic zone in developing growth plates, we assessed expression of vascular endothelial growth factor (*Vegf*) (24, 33, 34). As shown in long bones from 15.5-dpc embryos (Fig. 2*D*), expression of *Vegf*, using *in situ* hybridization, was limited to cells in the distal growth plates in WT mice but included cells in the entire primary center of ossification in *Mmp13*$^{-/-}$ mice. The observed pattern of CD31 staining in 15.5-dpc embryos (Fig. 2 *B* and *C*) is consistent with decreased vascular ingrowth and might be explained by sequestration of Vegf in the cartilage ECM as proposed by Vu *et al.* (24), to explain the phenotype of *Mmp9*$^{-/-}$ mice.

Persistent Abnormal Skeletal Phenotype in Adult *Mmp13*$^{-/-}$ Mice. We emphasize that the formation of primary ossification centers in the *Mmp13*$^{-/-}$mice, although delayed during embryonic development, began to normalize after birth. We found no gross abnormality in skull or spine of newborn mice. Abnormal growth plates were still present, however, in 4-wk-old mice and were associated with a tendency toward metaphyseal flaring and increased trabecular bone mass (data not shown). The *Mmp13*$^{-/-}$ femurs were also shorter than the WT femurs by $\approx$8%, measured in mice at ages 4 wk ($P < 0.01$) and 12 wk ($P < 0.001$). As shown in sections of distal femurs from 12-wk-old *Mmp13*$^{-/-}$ mice compared with WT mice (Fig. 5), there was persistent lengthening of growth plates, increased numbers of chondrocytes, and irregularly aligned chondrocyte columns as shown previously in embryos (Figs. 2*E* and 3).

Discussion

MMP13 (collagenase-3), a highly expressed collagenolytic MMP in developing bone and cartilage, has been assigned a role in the joint tissue destruction that is a major feature of various forms of human arthritis (3, 35, 36). We demonstrate here that a targeted null mutation in mouse *Mmp13* resulted in a profound embryonic and adult skeletal phenotype characterized by abnormal growth plates and delayed ossification. During embryonic development at the earliest stage examined, *Mmp13*$^{-/-}$ mice had growth plates in long bones almost double in length, accounted for by increases in the zone of hypertrophy. Among the processes that could account for increase in the hypertrophic zone are decreased proteolysis of the ECM, increased proliferation of chondrocytes in more proximal portions of growth plates, decreased apoptosis of the terminal hypertrophic chondrocytes and decreased resorption of calcified cartilage by cells entering with vascular ingrowth from the primary centers of ossification. Several of these potential mechanisms are operative in the Mmp13-deficient mice.

With regard to decreased proteolysis, we focused on collagens in the ECM in distal growth plates. Mmp13, produced by chondrocytes but not by osteoclasts/chondroclasts, is particularly effective in proteolysis of type II compared to type I collagen with a high V_{max} and low K_M (35). Using antibodies that detect epitopes in the specific proteolytic fragments, we obtained evidence for Mmp13 cleavage of type II collagen *in vivo* in WT mice but not in *Mmp13*$^{-/-}$ mice. It is thus unlikely that other Mmps compensate for the loss of Mmp13 function in cartilage. The delay in ossification so prominent in 15.5-dpc *Mmp13*$^{-/-}$ embryos is largely transient. *Mmp8* is clearly expressed in newborn *Mmp13*$^{-/-}$ and WT skeletons (37), and the faint signal in the primary centers of ossification that we detected in newborn *Mmp13*$^{-/-}$ mice by using the QRGIV TC^{B} cleavage fragment antibody could be ascribed to action of Mmp8, produced by hematopoietic cells, on type I collagen. Type X collagen is also a substrate for MMP1 and Mmp13 (38, 39). We found that the area of type X collagen deposition was significantly increased in growth plates from *Mmp13*$^{-/-}$ mice, consistent with decreased proteolysis. Thus, decreased proteolysis of cartilage ECM is the most likely explanation for our findings in *Mmp13*$^{-/-}$ mice. Nevertheless, because the area where *Col10a1* was expressed was also greater in *Mmp13*$^{-/-}$ mice, increased synthesis of type X collagen could also contribute. The expression of osteopontin, another molecular marker of chondrocyte hypertrophy (29, 30), was also increased in *Mmp13*$^{-/-}$ growth plates. Expanded domains of type X collagen and osteopontin have also been found in mice with targeted misexpression of *Dlx5*, a positive regulator of chondrocyte maturation (40).

Increased accumulation of type II collagen in the absence of functional Mmp13 and decreased collagen degradation could secondarily regulate development of the hypertrophic chondrocyte phenotype. An α_2-integrin-mediated interaction of osteoblasts with type I collagen is required for activation of *Osf2/Cbfa1/Runx2* and induction of osteoblast-specific gene expression in bone (41, 42). *Osf2/Cbfa1/Runx2* also acts as a chondrocyte differentiation factor (42–44). Type II and/or type X collagens might thus have roles in the regulation of cartilage-specific gene expression similar to those of type I collagen in the regulation of bone-specific gene expression. Further support for a regulatory role for Mmp13 comes from observations on *c-maf*-null mice (45). The transcription factor c-Maf is normally expressed in late hypertrophic chondrocytes and in 15.5-dpc *c-maf*-null embryos; intensity of *Mmp13* expression in these cells was markedly reduced. Thus, *Mmp13* could be a direct target of c-Maf (45). Later in development, however, when the hypertrophic domain was expanded, *Mmp13* expression normalized in the *c-maf*-null mice. Because we found increased numbers of hypertrophic chondrocytes in growth plates from *Mmp13*$^{-/-}$ mice, increased entry of cells into the hypertrophic chondrocyte pool is a possibility. The cyclin-dependent kinase inhibitor p57^{Kip2}, which normally participates in the coordination and differentiation of growth plate chondrocytes (46), might have a role. The metatarsal growth plates from 2-wk-old *Mmp9*$^{-/-}$ mice were markedly lengthened (24). Mmp9 is not a collagenase, however, and in our *Mmp13*$^{-/-}$ mice, growth plates were abnormal despite increased *Mmp9* expression. We tried terminal deoxynucleotidyltransferase-mediated dUTP nick end labeling staining (19) to assess apoptosis of hypertrophic chondrocytes but noted so few apoptotic cells in the distal growth plate in any of the mice

(data not shown) that apoptosis could not explain the differences in *Mmp13*$^{-/-}$ and WT mice.

Our observations are also consistent with altered vascular penetration into the primary centers of ossification in *Mmp13*$^{-/-}$ mice. Binding of Vegf by infusion of dimerized soluble receptor Flt-1 reversibly delayed formation of the primary spongiosa and increased the length of the hypertrophic zone of distal growth plates (33). Evidence was presented suggesting that Vegf was sequestered in the cartilage ECM of *Mmp9*$^{-/-}$ mice and unavailable to bind to its receptor on vascular endothelial cells (24). Decreased availability of Vegf in the absence of the proteolytic function of Mmp13 might also contribute to the widened growth plates. Defects in general postnatal angiogenesis as well as more specific vascularization of cartilage have been described in *Mmp14*$^{-/-}$ mice where hypertrophic zones in growth plates are also lengthened (25, 26). An aspect of the phenotype in the *Mmp14*$^{-/-}$ mice that was not observed in the *Mmp13*$^{-/-}$ mice was abnormal vascularization of the epiphyses and delayed formation of secondary centers of ossification. Mmp14 deficiency might result in failure to activate proMmp13 through a proteolytic cascade also involving Mmp2 (26). Defects in vascularization might therefore contribute to the delayed osteoclast migration observed in the *Mmp13*$^{-/-}$ mice because, despite normal or increased *Mmp9* and *Mmp14* expression, osteoclast penetration is clearly retarded.

Based on our results, Mmp13 has a critical role in regulating events in the growth plate beginning in embryonic development. Deficiency of Mmp13 with failure to normally resorb collagens in the cartilage ECM profoundly affects cellular activities that underlie differentiation of hypertrophic chondrocytes that persist in newborn and adult mice. The phenotype of adult *Mmp13*$^{-/-}$ mice with increased length of growth plates, increased numbers of chondrocytes, and distortion of alignment of the rows of chondrocytes thus has features of a chondrodysplasia. It is pertinent that a form of human chondrodysplasia, the Missouri variant of spondyloepimetaphyseal dysplasia (47), is caused by a mutation in *MMP13*.‖

‖Kennedy, A. M., Christie, P. T., Harding, B., Pannett, A. A. J., Dearlove, A., Whyte, M. P. & Thakker, R. V. (2002) *J. Bone Miner. Res.* **17,** Suppl 1., S175 (abstr.).

We thank Dr. En Li and the Massachusetts General Hospital Transgenic Core Service for help with the *Mmp13* knockout procedures, Dr. Ernestina Schipani (Endocrine Unit, Massachusetts General Hospital) for help with *in situ* hybridization, and Dr. Eunice Lee for the generous gift of the antibody to the QRGIV sequence in collagens. This work was supported by a Schering Fellowship from the Japanese Menopause Society (to M.I.), European Union Grant FP6-CancerDegradome (to C.L.-O.), and National Institutes of Health Grants RO1AR44815 and P50AR44855 (to S.M.K.).

1. Nagase, H. & Woessner, J. F., Jr. (1999) *J. Biol. Chem.* **274,** 21491–21494.
2. Sternlicht, M. D. & Werb, Z. (2001) *Annu. Rev. Cell Dev. Biol.* **17,** 463–516.
3. Murphy, G., Knäuper, V., Atkinson, S., Butler, G., English, W., Hutton, M., Stracke, J. & Clark, I. (2002) *Arthritis Res.* **4,** Suppl. 3, S39–S49.
4. Stamenkovic, I. (2003) *J. Pathol.* **200,** 448–464.
5. Mattot, V., Raes, M. B., Henriet, P., Eeckhout, Y., Stehelin, D., Vandenbunder, B. & Desbiens, X. (1995) *J. Cell Sci.* **108,** 529–535.
6. Fuller, K. & Chambers, T. J. (1995) *J. Cell Sci.* **108,** 2221–2230.
7. Gack, S., Vallon, R., Schmidt, J., Grigoriadis, A., Tuckermann, J., Schenkel, J., Weiher, H., Wagner, E. F. & Angel, P. (1995) *Cell Growth Differ.* **6,** 759–767.
8. Stähle-Backdahl, M., Sandstedt, B., Bruce, K., Lindahl, A., Jimenez, M. G., Vega, J. A. & López-Otín, C. (1997) *Lab. Invest.* **76,** 717–728.
9. Aimes, R. T. & Quigley, J. P. (1995) *J. Biol. Chem.* **270,** 5872–5876.
10. Seandel, M., Noack-Kunnmann, K., Zhu, D., Aimes, R. T. & Quigley, J. P. (2001) *Blood* **97,** 2323–2332.
11. Ohuchi, E., Imai, K., Fujii, Y., Sato, H., Seiki, M. & Okada, Y. (1997) *J. Biol. Chem.* **272,** 2446–2451.
12. Balbín, M., Fueyo, A., Knäuper, V., López, J. M., Álvarez, J., Sánchez, L. M., Quesada, V., Bordallo, J., Murphy, G. & López-Otín, C. (2001) *J. Biol. Chem.* **276,** 10253–10262.
13. Gross, J. (1981) in *Cell Biology of the Extracellular Matrix*, ed. Hay, E. D. (Plenum, New York), pp. 217–258.
14. Selvamurugan, N., Pulumati, M. R., Tyson, D. R. & Partridge, N. C. (2000) *J. Biol. Chem.* **275,** 5037–5042.
15. Jimenez, M. J., Balbín, M., López, J. M., Alvarez, J., Komori, T. & López-Otín, C. (1999) *Mol. Cell. Biol.* **19,** 4431–4442.
16. Porte, D., Tuckermann, J., Becke, M., Baumann, B., Teurich, S., Higgins, T., Owen, M. J., Schorpp-Kistner, M. & Angel, P. (1999) *Oncogene* **18,** 667–678.
17. Krane, S. M., Byrne, M. H., Lemaitre, V., Henriet, P., Jeffrey, J. J., Witter, J. P., Liu, X., Wu, H., Jaenisch, R. & Eeckhout, Y. (1996) *J. Biol. Chem.* **271,** 28509–28515.
18. Otterness, I. G., Downs, J. T., Lane, C., Bliven, M. L., Stukenbrok, H., Scampoli, D. N., Milici, A. J. & Mezes, P. S. (1999) *Matrix Biol.* **18,** 331–341.
19. Zhao, W., Byrne, M. H., Wang, Y. & Krane, S. M. (2000) *J. Clin. Invest.* **106,** 941–949.
20. Zhao, W., Byrne, M. H., Boyce, B. F. & Krane, S. M. (1999) *J. Clin. Invest.* **103,** 517–524.
21. Kusano, K., Miyaura, C., Inada, M., Tamura, T., Ito, A., Nagase, H., Kamoi, K. & Suda, T. (1998) *Endocrinology* **139,** 1338–1345.
22. Miyaura, C., Inada, M., Suzawa, T., Sugimoto, Y., Ushikubi, F., Ichikawa, A., Narumiya, S. & Suda, T. (2000) *J. Biol. Chem.* **275,** 19819–19823.
23. Engsig, M. T., Chen, Q. J., Vu, T. H., Pedersen, A. C., Therkidsen, B., Lund, L. R., Henriksen, K., Lenhard, T., Foged, N. T., Werb Z, *et al.* (2000) *J. Cell Biol.* **151,** 879–889.
24. Vu, T. H., Shipley, J. M., Bergers, G., Berger, J. E., Helms, J. A., Hanahan, D., Shapiro, S. D., Senior, R. M. & Werb, Z. (1998) *Cell* **93,** 411–422.
25. Holmbeck, K., Bianco, P., Caterina, J., Yamada, S., Kromer, M., Kuznetsov, S. A., Mankani, M., Robey, P. G., Poole, A. R., Pidoux, I., *et al.* (1999) *Cell* **99,** 81–92.
26. Zhou, Z., Apte, S. S., Soininen, R., Cao, R., Baaklini, G. Y., Rauser, R. W., Wang, J., Cao, Y. & Tryggvason, K. (2000) *Proc. Natl. Acad. Sci. USA* **97,** 4052–4057.
27. Linsenmayer, T. F., Chen, Q. A., Gibney, E., Gordon, M. K., Marchant, J. K., Mayne, R. & Schmid, T. M. (1991) *Development (Cambridge, U.K.)* **111,** 191–196.
28. Warman, M. L., Abbott, M., Apte, S. S., Hefferon, T., McIntosh, I., Cohn, D. H., Hecht, J. T., Olsen, B. R. & Francomano, C. A. (1993) *Nat. Genet.* **5,** 79–82.
29. Gerstenfeld, L. C. & Shapiro F. D. (1996) *J. Cell. Biochem.* **62,** 1–9.
30. Koyama, E., Golden, E. B., Kirsch, T., Adams, S. L., Chandraratna, R. A., Michaille, J. J. & Pacifici, M. (1999) *Dev. Biol.* **208,** 375–391.
31. Kronenberg, H. M. (2003) *Nature* **423,** 332–336.
32. Ingham, P. W. & McMahon, A. P. (2001) *Genes Dev.* **15,** 3059–3087.
33. Gerber, H. P., Vu, T. H., Ryan, A. M., Kowalski, J., Werb, Z. & Ferrara, N. (1999) *Nat. Med.* **5,** 623–628.
34. Zelzer, E., McLean, W., Ng, Y. S., Fukai, N., Reginato, A. M., Lovejoy, S., D'Amore, P. A. & Olsen, B. R. (2002) *Development (Cambridge, U.K.)* **129,** 1893–1904.
35. Mitchell, P. G., Magna, H. A., Reeves, L. M., Lopresti-Morrow, L. L., Yocum, S. A., Rosner, P. J., Geoghegan, K. F. & Hambor, J. E. (1996) *J. Clin. Invest.* **97,** 761–768.
36. Neuhold, L. A., Killar, L., Zhao, W., Sung, M. L., Warner, L., Kulik, J., Turner, J., Wu, W., Billinghurst, C., Meijers, T., *et al.* (2001) *J. Clin. Invest.* **107,** 35–44.
37. Sasano, Y., Zhu, J. X., Tsubota, M., Takahashi, I., Onodera, K., Mizoguchi, I. & Kagayama, M. (2002) *J. Histochem. Cytochem.* **50,** 325–332.
38. Schmid, T. M., Mayne, R., Jeffrey, J. J. & Linsenmayer, T. F. (1986) *J. Biol. Chem.* **261,** 4184–4189.
39. Welgus, H. G., Fliszar, C. J., Seltzer, J. L., Schmid, T. M. & Jeffrey, J. J. (1990) *J. Biol. Chem.* **265,** 13521–13527.
40. Ferrari, D. & Kosher, R. A. (2002) *Dev. Biol.* **252,** 257–270.
41. Xiao, G., Wang, D., Benson, M. D., Karsenty, G. & Franceschi, R. T. (1998) *J. Biol. Chem.* **273,** 32988–32994.
42. Enomoto, H., Enomoto-Iwamoto, M., Iwamoto, M., Nomura, S., Himeno, M., Kitamura, Y., Kishimoto, T. & Komori, T. (2000) *J. Biol. Chem.* **275,** 8695–8702.
43. Takeda, S., Bonnamy, J. P., Owen, M. J., Ducy, P. & Karsenty, G. (2001) *Genes Dev.* **15,** 467–481.
44. Ueta, C., Iwamoto, M., Kanatani, N., Yoshida, C., Liu, Y., Enomoto-Iwamoto, M., Ohmori, T., Enomoto, H., Nakata, K., Takada, K., *et al.* (2001) *J. Cell Biol.* **153,** 87–100.
45. MacLean, H. E., Kim, J. I., Glimcher, M. J., Wang, J., Kronenberg, H. M. & Glimcher, L. H. (2003) *Dev. Biol.* **262,** 51–63.
46. Yan, Y., Frisén, J., Lee, M. H., Massagué, J. & Barbacid, M. (1997) *Genes Dev.* **11,** 973–983.
47. Patel, A. C., McAlister, W. H. & Whyte, M. P. (1993) *Medicine* **72,** 326–342.